



Cite this article: Wang Z, Dai M, Wang Y, Cooper KL, Zhu T, Dong D, Zhang J, Zhang S. 2014 Unique expression patterns of multiple key genes associated with the evolution of mammalian flight. *Proc. R. Soc. B* **281**: 20133133.
<http://dx.doi.org/10.1098/rspb.2013.3133>

Received: 29 November 2013

Accepted: 10 March 2014

Subject Areas:

evolution, developmental biology, genomics

Keywords:

bat wing, mRNA-Seq, 5'HoxD, *Tbx3*, *Fam5c*

Authors for correspondence:

Shuyi Zhang

e-mail: syzhang@bio.ecnu.edu.cn

Zhe Wang

e-mail: zwang@sat.ecnu.edu.cn

[†]These authors are co-first authors.

Electronic supplementary material is available at <http://dx.doi.org/10.1098/rspb.2013.3133> or via <http://rspb.royalsocietypublishing.org>.

Unique expression patterns of multiple key genes associated with the evolution of mammalian flight

Zhe Wang^{1,†}, Mengyao Dai^{1,†}, Yao Wang¹, Kimberly L. Cooper^{2,3}, Tengteng Zhu¹, Dong Dong¹, Junpeng Zhang¹ and Shuyi Zhang¹

¹Institute of Molecular Ecology and Evolution (iAIR), East China Normal University, Shanghai 200062, People's Republic of China

²Division of Biological Sciences, University of California, San Diego, CA 92093, USA

³Department of Genetics, Harvard Medical School, Boston, MA 02115, USA

Bats are the only mammals capable of true flight. Critical adaptations for flight include a pair of dramatically elongated hands with broad wing membranes. To study the molecular mechanisms of bat wing evolution, we perform genomewide mRNA sequencing and *in situ* hybridization for embryonic bat limbs. We identify seven key genes that display unique expression patterns in embryonic bat wings and feet, compared with mouse fore- and hindlimbs. The expression of all 5'HoxD genes (*Hoxd9–13*) and *Tbx3*, six known crucial transcription factors for limb and digit development, is extremely high and prolonged in the elongating wing area. The expression of *Fam5c*, a tumour suppressor, in bat limbs is bat-specific and significantly high in all short digit regions (the thumb and foot digits). These results suggest multiple genetic changes occurred independently during the evolution of bat wings to elongate the hand digits, promote membrane growth and keep other digits short. Our findings also indicate that the evolution of limb morphology depends on the complex integration of multiple gene regulatory networks and biological processes that control digit formation and identity, chondrogenesis, and interdigital regression or retention.

1. Introduction

Bats are the only mammals naturally capable of powered and sustained flight, and achieve this flight using wings [1]. Unlike the avian wing with feathers, the bat wing is supported by four elongated digits within the wing membrane (figure 1*b*). While the four posterior fingers (forelimb digits II–V) of bats are dramatically elongated, the thumb (forelimb digit I) and hindlimb digits remain short and are similar in length and width to each other [2]. The longest finger, forelimb digit III, is 1.54 times as long as the head–body length in the common bent-wing bat (*Miniopterus schreibersii*). In contrast, its thumb and hindlimb digits are only 0.09 and 0.14 times relative to the head–body length. In mouse and human, the longest finger or foot digit is no more than 0.17 (0.08–0.17) times relative to the head–body length (figure 2*a*). This highlights the impressive fact that the longest bat finger is more than nine times the proportionate length of a human finger.

We hypothesized that the dramatic morphological change in bat forelimb required a combination of changes in the expression of many genes [3]. However, so far, targeted candidate gene approaches have identified only seven genes with differences in expression in bat forelimb compared with hindlimb and mouse limbs during development. Only two of these are transcription factors that may play an upstream and regulatory role for bat wing development [4–9]. Thus, the full complexity of the mechanism of bat wing evolution remains to be shown, and the key differentially expressed genes contributing to this unique morphology remain to be identified.

We have taken a genomewide approach to investigate how the transcription profiles were altered during bat wing evolution. We performed a transcriptome

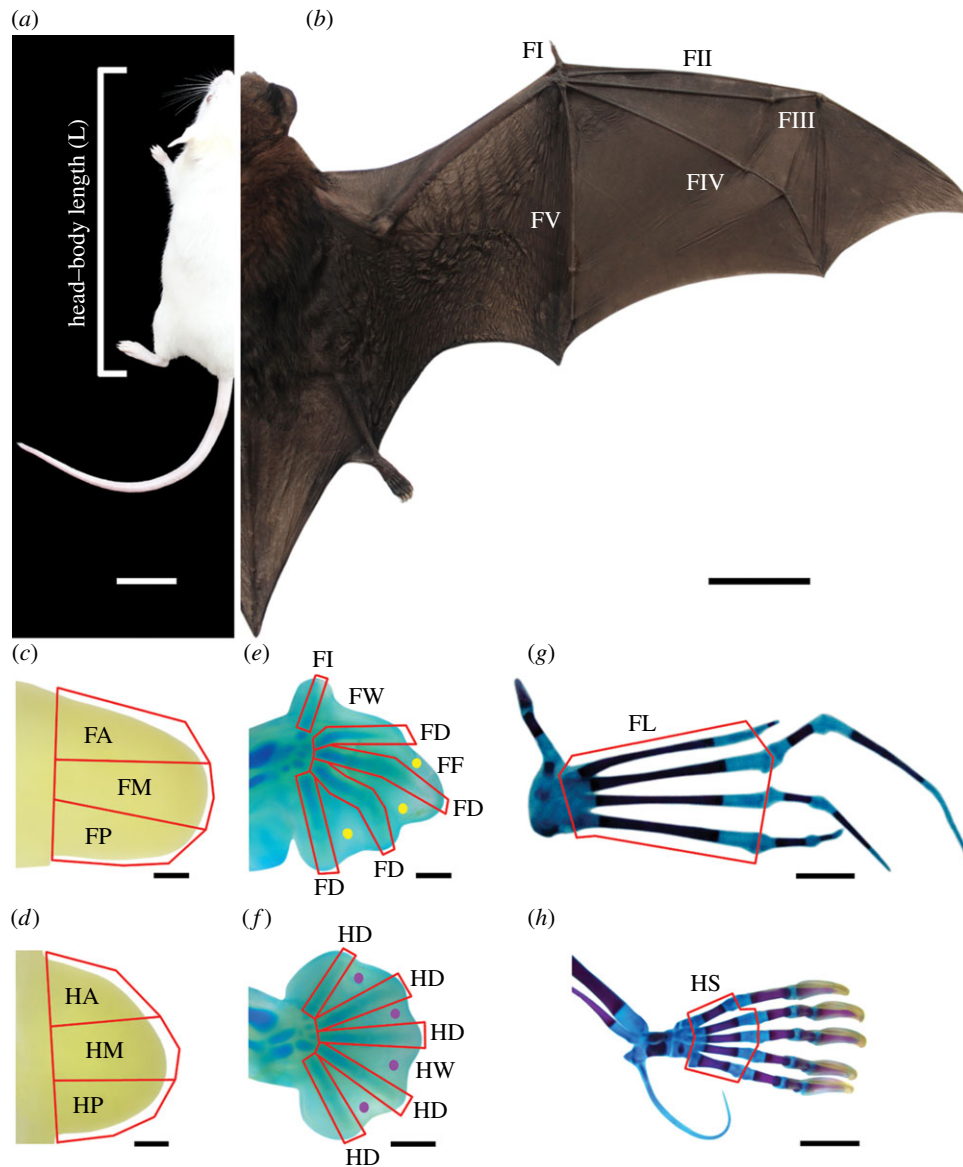


Figure 1. Morphological comparison and sampling positions for mRNA-Seq. (a,b) Morphology of adult mouse and bat (*M. schreibersii*) limbs. (c–h) Sampling positions for mRNA-Seq. Samples are enclosed by red lines, except for the interdigital tissues at stage 17. (c,d) Stage 14. (e,f) Early stage 17. (g,h) Middle fetal stage. The dorsal view of the autopod is shown with anterior up and distal to the right. FI, FII, FIII, FIV and FV: forelimb digits I, II, III, IV and V; FA, FM, FP, HA, HM and HP: anterior (A), middle (M) and posterior (P) parts of the fore- (F) and hindlimb (H) buds; FW: interdigital tissue between forelimb digits I and II; FD: forelimb digits II–V; FF (yellow dots): interdigital tissues between forelimb digits II and V; HD: hindlimb digits I–V; HW (purple dots): interdigital tissues between hindlimb digits I and V; FL: metacarpals of forelimb digits II–V; HS: metatarsals of hindlimb digits I–V. Scale bars, 2 cm in (a,b), 200 μm in (c,d), 500 μm in (e,f) and 2 mm in (g,h).

sequencing approach (mRNA-Seq) for bat's fore- and hindlimbs at a series of developmental stages. We validated these results in comparison with other mammals by *in situ* hybridization (ISH) for embryonic bats and mice. Finally, through these analyses, we have identified a subset of highly differentially expressed genes that include six important transcription factors for limb development that likely play a role in the evolution of the unique forelimb morphology of bats.

2. Material and methods

(a) Sample collection

Common bent-wing bats (*M. schreibersii*) were captured from a cave at Anhui province of China (30°20.263' N, 117°50.180' E) from May to June 2012. For mRNA-Seq, six samples (FA, FM, FP, HA, HM and HP) were collected from anterior, middle and

posterior parts of the fore- and hindlimb buds of three individuals at stage 14 (figure 1c,d). Another six samples (FI, FW, FD, FF, HD and HW) were collected from eight individuals at stages 15–17, when the forelimb digit became elongating and the interdigital tissues had not disappeared in the hindlimb. These samples are forelimb digit I (FI), interdigital tissue between forelimb digits I and II (FW), the elongating forelimb digits II–V (FD), interdigital tissues between forelimb digits II and V (FF), hindlimb digits I–V (HD) and interdigital tissues between hindlimb digits I and V (HW; figure 1e,f). The last two samples (FL and HS) were collected from the elongating metacarpals of forelimb digits II–V (FL) and the metatarsals of hindlimb digits I–V (HS) of three individuals at middle fetal stage (figure 1g,h).

(b) Identifying embryonic stages

Bat and mouse embryonic stages are identified according to previous studies [10–12]. Because of differences in species, pregnancy duration and the heterochrony of forelimb and hindlimb, it is

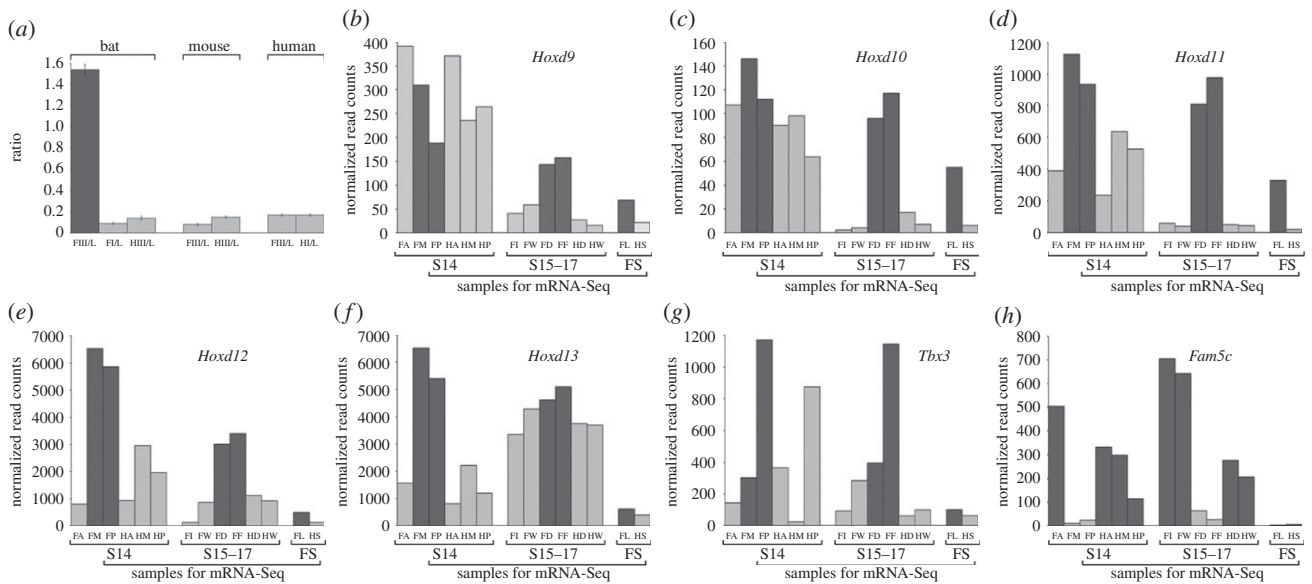


Figure 2. Comparison of digit lengths in different species and expression levels of *Hoxd9–13*, *Tbx3* and *Fam5c* in mRNA-Seq samples. (a) Ratios of digit length relative to head–body length (L) in the bat, mouse and human. FI, FIII: forelimb digits I and III; HI, HIII: hindlimb digits I and III. Error bars, mean \pm s.d. ($n = 15$). (b–h) Expression levels of *Hoxd9–13*, *Tbx3* and *Fam5c* in mRNA-Seq samples. Symbols of the samples as in figure 1. S14: stage 14; S15–17: stages 15–17; FS, fetal stage.

challenging to define exact equal stages between two species that are from two different orders. However, we can give a rough corresponding stage of mice to bats by taking the following five factors into consideration (i) overall appearance of the autopod; (ii) digit condensation (electronic supplementary material, figure S1); (iii) the number of phalanges (electronic supplementary material, figure S1); (iv) regression of interdigital tissues and (v) appearance of claw primordia or keratinized claws. We also consulted and compared with other relevant studies [12,13].

(c) mRNA-Seq and data analysis

Total RNA was extracted using the RNeasy mini kit (Qiagen), and treated with DNase I using RNase-free DNase set (Qiagen). TruSeq RNA sample prep kit (Illumina), TruSeq PE cluster kit (Illumina) and TruSeq SBS kit (Illumina) were used for constructing libraries, cluster amplification and final sequencing-by-synthesis. mRNA sequencing (mRNA-Seq) was performed using a HiSeq-2000 sequencing system (Illumina). Image analysis, base calling and extraction of 100 bp pair-end reads were performed using the Illumina pipeline. The transcriptome sequences were de novo assembled using Trinity package [14,15]. Assembled contigs were searched using BLASTX against the NCBI non-redundant nucleotide database with an E -value threshold of 1×10^{-5} . The resulting best blast hits were extracted, and coding sequences were subsequently determined. Read counts of all genes were then estimated using RSEM software in the Trinity package [16]. Normalization of gene counts (i.e. gene expression levels) and differential expression analysis were performed by the methods we described previously [17]. Briefly, data were normalized by the trimmed mean of M values (TMM) method using the edgeR package [18,19], and the DEGseq package [20] was used to identify differentially expressed genes between samples. The cut-off of significantly differential expression is a q -value [21] less than 0.0001.

(d) *In situ* hybridization

The procedure and reagents used for ISH are the same as we described previously [17]. Briefly, total RNA was extracted from bat (*M. schreibersii*) and mouse (*Mus musculus*) embryos, and then cDNA was synthesized from the total RNA. Primers used for amplifying investigated genes are shown in the electronic

supplementary material, table S1. PCR products were purified and cloned into pGEM-T vector. ISH probes were synthesized by linearizing the plasmid with enzyme and transcribing with T7 or SP6 polymerase, labelled with digoxigenin, and hybridized with embryos at 70°C.

3. Results

(a) Significant differential expression of seven major genes in bat fore- and hindlimbs

Bat forelimb digits condense at approximately stage 15 and elongate during subsequent stages [10] (electronic supplementary material, figure S1). To find genes likely to contribute to digit elongation, we applied mRNA-Seq to bat fore- and hindlimb digits at stages 15–17. We compared the mRNA-Seq data of the elongating forelimb digits with that of digits that remain short (thumb and hindlimb digits; figure 1*e,f*). We identified 426 genes that are expressed at a significantly higher level in the elongating forelimb digits than in the short digits, and 532 genes that are expressed at a significantly higher level in the short digits than in the elongating forelimb digits ($q < 0.0001$). To limit subsequent analysis to those key genes that may play a prominent role in evolution of morphology, we sorted the genes by expression fold change and looked for genes with high expression in the elongating or short digits. Among the 30 genes with changes over fourfold, we found a set of transcription factors important for limb development; *Hoxd9–12* and *Tbx3* are in the top eight genes that are expressed at a significantly higher level in the elongating forelimb digits than in the short digits, and *Fam5c* is the top gene that is expressed at a significantly higher level in the short digits than in the elongating forelimb digits (figure 2). Although the expression fold change of *Hoxd13* is 1.32, it is expressed at a significantly higher level in the elongating forelimb digits than in the short digits ($q < 0.0001$; figure 2*f*).

We also analysed the mRNA-Seq data of these genes at stage 14 (limb bud stage) and at the fetal stage (figure 1*c,d,g,h*). Before

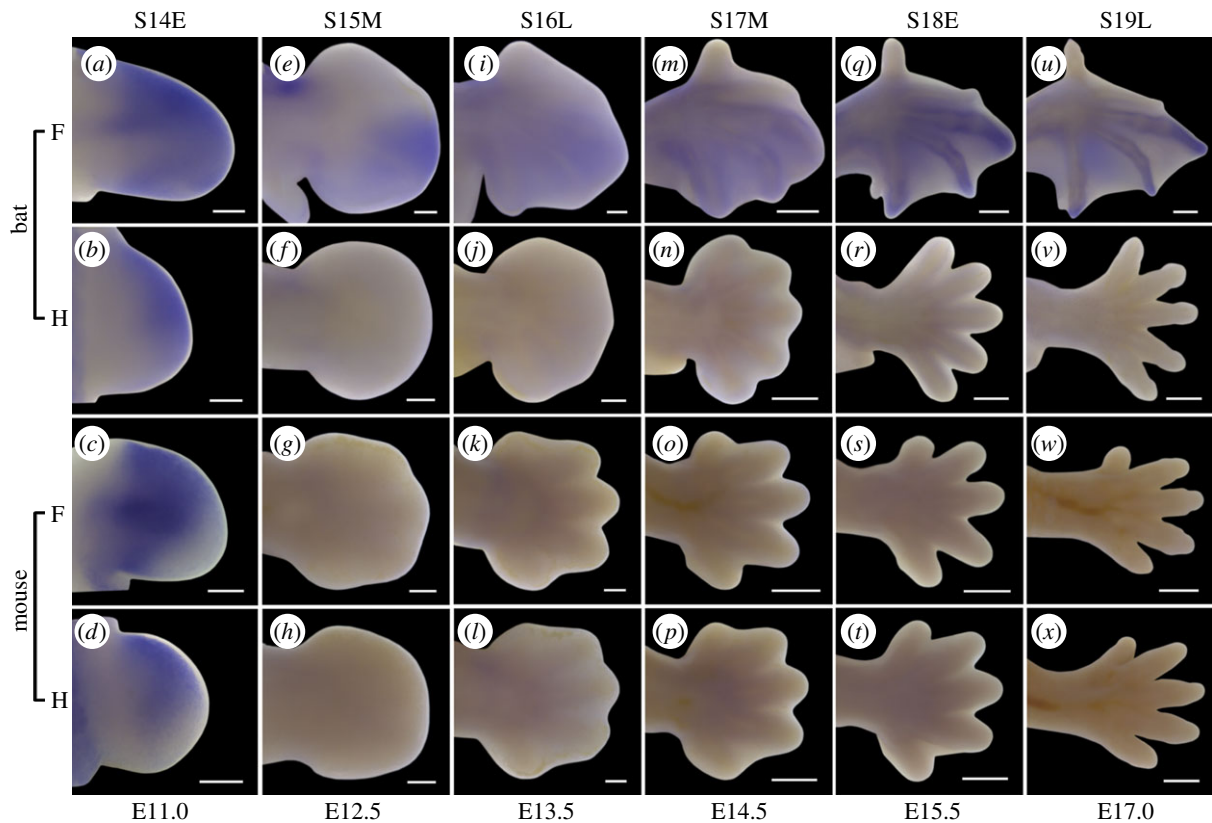


Figure 3. *Hoxd9* expression in the fore- (F) and hindlimbs (H) of embryonic bats and mice visualized by ISH. Orientation of limbs as in figure 1. Scale bars, 200 μm in (a–l) and 500 μm in (m–x).

digit condensation, *Hoxd10–13* and *Tbx3* are already significantly highly expressed in the middle and posterior regions of the forelimb bud where elongated digits will form, compared with the corresponding regions of the hindlimb bud (figure 2). *Fam5c* is already significantly highly expressed in the forelimb anterior region and the entire hindlimb bud, where the short digits will develop, compared with regions where the rapidly elongating digits will form (figure 2h). In the middle of fetal stage, when all digits have begun to calcify and claws are formed, *Hoxd9–13* genes are still significantly highly expressed in the elongating metacarpals II–V compared with the metatarsals (figure 2).

(b) Prolonged and high expression of 5'*HoxD* genes in the elongating wing area

To validate the mRNA-Seq results and understand the evolution of spatio-temporal expression of 5'*HoxD* genes in the bat relative to a mammal with a more generalized limb morphology, we performed ISH in the common bent-wing bat and mouse at a continuous series of embryonic stages. The results are consistent with the mRNA-Seq data and show that expression of *Hoxd9–13* is much higher and prolonged in the elongating wing area compared with the bat thumb, hindlimbs, and mouse fore- and hindlimbs. In bats, *Hoxd9–11* are highly expressed in hand digits II–V and their interdigital tissues from stage 14 to late stage 19, but expressed in the bat foot only at stage 14 (figure 3 and the electronic supplementary material, figures S2 and S3). *Hoxd12* is highly expressed in hand digits II–V and their interdigital tissues from late stage 14 to late stage 19, but hardly expressed in the bat foot from late stage 17 to late stage 19 (electronic supplementary material, figure S4). The expression dose and area of *Hoxd9–12* in the foot

are lower and smaller than those in the hand (figure 3 and the electronic supplementary material, figures S2 and S4). The expression patterns of *Hoxd13* in bat limbs before stage 16 have been previously described in another bat species, *Carollia perspicillata* [6]. In this study, we find that *Hoxd13* is highly expressed in hand digits II–V from early stage 18 to middle stage 19, but weakly expressed in the bat foot at early stage 18 and nearly not expressed in the bat foot from late stage 18 to middle stage 19 (electronic supplementary material, figure S5). In mice, *Hoxd9* is only expressed in both limb buds at E11.0, corresponding to bat early stage 14, and not expressed in either hand or foot afterwards (figure 3). *Hoxd10–13* are expressed in both hand and foot from E11.5 to E15.0, corresponding to bat stages 14–17, but weakly expressed at E15.5 and nearly not expressed afterwards (electronic supplementary material, figures S2–S5). It is interesting that the expression levels of *Hoxd10* and *Hoxd11* are much higher in the bat hand plate than those in the bat foot plate and in both limbs of the mouse at bat stage 15 (corresponding to mouse E12.5), showing a transient elevation in the expression dose (electronic supplementary material, figures S2 and S3).

(c) Prolonged and high expression of *Tbx3* in the posterior wing area

To validate the mRNA-Seq data and compare the expression pattern of *Tbx3* in bat limbs with that of mouse limbs, we performed ISH in the common bent-wing bat and mouse at a continuous series of embryonic stages. The results are consistent with the mRNA-Seq data and show that expression of *Tbx3* is much higher and prolonged until late stage 19 throughout the elongating wing area compared with the bat thumb, hindlimbs and mouse fore- and hindlimbs (electronic supplementary

material, figure S6). In mouse, the expression of *Tbx3* is largely restricted to the margin of autopods and hardly expressed at the interdigital tissues of both limbs as it is in the bat wing (electronic supplementary material, figure S6).

Although the expressions of *Tbx3* and 5'HoxD genes are all prolonged in the bat wing, the expression of *Tbx3* is different from that of 5'HoxD genes in two aspects. First, the expression region of *Tbx3* is more posterior than that of 5'HoxD genes. It is highly expressed in bat interdigital tissues between forelimb digits III and V, weakly expressed in bat interdigital tissues between forelimb digits I and III, and hardly expressed in the interdigital regions of bat hindlimbs and mouse fore- and hindlimbs in all embryonic stages (electronic supplementary material, figure S6). Additionally, *Tbx3* expression is maintained in interdigital regions and in the perichondrium of bat forelimbs throughout the investigated stages, whereas the expressions of *Hoxd9–13* are reduced in the interdigital tissue and concentrated in the perichondrium of the elongating digits after stage 16 (figure 3 and electronic supplementary material, figures S2–S6).

(d) Unique and bat-specific expression of *Fam5c* in bat short digit area

The results of ISH for *Fam5c* are consistent with the mRNA-Seq data and show more detailed expression domains of this gene. In the forelimb, it first appears at the anterior and middle margin of the limb bud in early stage 14, and then retreats to the anterior border of the limb bud in middle stage 14 (electronic supplementary material, figure S7a,c). When digits are condensing in the forelimb at stage 15, *Fam5c* is highly expressed at the distal ends of the thumb and its immediate interdigital tissue, decreasingly expressed at the margin of interdigital tissue between digits II and III, with no expression posteriorly (electronic supplementary material, figure S7e,g). In the hindlimb, *Fam5c* is first expressed weakly at the anterior margin of the limb bud in early stage 14, and then increasingly expressed from the anterior to the posterior margin of the limb bud and foot plate, and finally highly expressed throughout the border of the entire foot plate at the end of stage 15 (electronic supplementary material, figure S7b,d,f,h). The expression of *Fam5c* nearly disappears in both fore- and hindlimbs in stage 16, but comes back at the tip and the forming articulations of the thumb and all the hindlimb digits, as well as the articulations of forelimb digit V, in stage 17 (electronic supplementary material, figures S7i–l and S1e,f). From stage 18 to 19, its expression is obviously present at the tips of all the foot digits and faintly at the tip of the thumbs (electronic supplementary material, figure S7m–p). In contrast to diverse expression in bat limb, we did not detect any expression of *Fam5c* in mouse limbs, but in the brain as previously reported [22].

4. Discussion

Hoxd10–13 are important transcription factors for autopod development and determining digit identity and morphology [23–25]. In mouse, loss of 5'HoxD genes results in a reduction in digit length, whereas increasing the expression of *Hoxd11* by gene duplication causes an increase in digit length [26–28]. Moreover, Zakany *et al.* [29] have shown that 5'HoxD genes regulate digit length in a dose-dependent

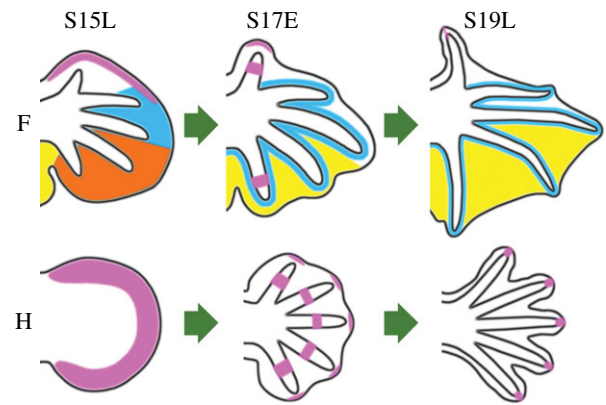


Figure 4. Schematic diagram of unique expression patterns of the genes investigated in this study during bat limb development. 5'HoxD genes (blue and orange) are highly expressed in interdigital regions and in the perichondrium of hand digits II–V in early stages, and then reduced in the interdigital tissue and concentrated in the perichondrium of the elongating digits after stage 16. *Tbx3* expression (yellow and orange) is highly expressed and maintained in the interdigital regions and in the perichondrium of forelimbs throughout the investigated stages. *Fam5c* (pink) is highly expressed at the distal ends of the thumb and its immediate interdigital tissue and throughout the border of the entire foot plate at late stage 15 (S15L). Then, *Fam5c* nearly disappears in both fore- and hindlimbs in stage 16, but comes back at the tip and the forming articulations of the thumb and all the hindlimb digits, as well as the articulations of forelimb digit V in early stage 17 (S17E). At late stage 19 (S19L), *Fam5c* expression is obviously present at the tips of all the foot digits and faintly at the tip of thumb. Orientation of limbs as in figure 1. F, forelimb; H, hindlimb.

manner. Our results are consistent with a hypothesis that higher levels of HoxD gene expression promote digit elongation in bats. Although *Hoxd9* deletion in mouse produces no measurable phenotype in the digits, there is a reduction in the humerus length suggesting a role in endochondral skeletal growth [30,31]. Our previous Tag-Seq study on another bat species (*Myotis ricketti*) predicted that *Hoxd9*, as well as *Tbx3*, are expressed at significantly higher levels in the elongating hand than in the foot at the fetal stage [32], supporting the hypothesis that these genes display similar expression patterns throughout the bat lineage. Although the expression fold change of *Hoxd13* is low after stage 14, even a slight dose change of this gene can readily affect the length of limb segments, including digits [30]. Thus, our findings of unique expression patterns of *Hoxd9–13* suggest an integral role of these genes for bat digit elongation.

Hockman *et al.* [8] found that a second wave of *Shh* expression in the interdigital membrane of bat forelimb at early stage 16. Because 5'HoxD genes can induce *Shh* expression in limbs [23,33], we propose that the short-term re-initiation of *Shh* expression in bat wing is caused by the significantly high expression of 5'HoxD genes at stages 15–16, especially the transient elevation in the expression dose of *Hoxd10* and *Hoxd11* at stage 15. Our previous study and Liang *et al.* did not find positive selection acting on the coding sequences of any 5'HoxD genes in the common ancestor of bats, suggesting that functions of these genes are important and conserved [34,35]. Our finding of prolonged and high expression of 5'HoxD genes in bat wings suggests a strong positive selection acted on enhancers to alter their expression patterns during wing formation in bat ancestors. Mutations in the HoxD limb enhancer, the global control region, may underlie lengthening of the bat wing digits [36].

In chicken, transient expression of *Tbx3* was detected at interdigital regions of foot digits in stages 27–30, corresponding to bat stages 15–17. However, this expression is weaker and shorter than that in the bat forelimb [37,38]. The difference between the expression of 5'HoxD genes and *Tbx3* in bat wings suggests that these genes may play different roles in bat wing formation, especially at late embryonic stages. Studies have shown that *Tbx3* can suppress apoptosis and promote cell proliferation in a variety of cell lines and organs [39–42], suggesting an important role in inhibiting the regression of forelimb interdigital tissues and promoting the growth of wing membranes in bats. In addition, *Tbx3* can specify posterior digit identity and suppress osteoblast differentiation [38,43], suggesting a possible contribution to elongating the posterior fingers by promoting chondrocyte proliferation and delaying osteoblast differentiation.

Fam5c, also known as *Brinp3*, was originally identified in mouse brain in 2004 [22]. The expression and function of this gene in limb development have not been reported. The bat-specific expression of *Fam5c* in limbs suggests that this gene has evolved specific functions for bat autopod development. *Fam5c* is a crucial soluble bone anabolic factor that is produced from muscle cells and promotes osteoblast differentiation and mineralization of osteoblasts [44]. In addition, *Fam5c* was identified as a tumour suppressor in tongue squamous cell carcinoma, and its methylation rates increased in gastric cancer [45,46]. Thus, its high expression in the region of bat short digits (the thumb and foot digits) potentially restricts endochondral growth and promotes osteoblast differentiation.

In conclusion, the data presented here reveal that changes in the expression patterns of multiple key genes correspond to the morphological changes during bat wing evolution. These genes function in three distinct areas of limb development (figure 4). First, 5'HoxD genes are highly expressed for a longer duration in the perichondrium of rapidly elongating digits. Second, *Tbx3* is highly expressed for a longer period of time in the tissue that forms the interdigital wing membranes. Finally, *Fam5c* is highly expressed in the thumb and hindlimb digits that remain short. Together, these genes and their distinct biological functions support a model whereby the evolution of bat wing morphology proceeded through the integrated control of a complex set of gene regulatory mechanisms impacting varied aspects of tissue morphology.

All procedures involving animals were carried out in accordance with the Policy on the Care and Use of Animals, approved by the Ethical Committee, Institute of Molecular Ecology and Evolution, East China Normal University.

Acknowledgements. We thank G. Zhu, F. Meng, and L. Fang for the assistance of fieldwork and experiments. We also thank people from Majorbio for the mRNA sequencing and assistance of data analysis.

Data accessibility. mRNA-Seq data: Gene Expression Omnibus (GEO) database accession number GSE50699.

Funding statement. This work was supported by grants from the National Natural Science Foundation of China (no. 31301191, 31172077, 91120001), the State Education Ministry of China (SRF for ROCS), Science and Technology Commission of Shanghai Municipality (No. 13ZR1412700) and East China Normal University.

References

- Swartz SM, Iriarte-Diaz J, Riskin DK, Breuer KS. 2012 A bird? A plane? No, it's a bat: an introduction to the biomechanics of bat flight. In *Evolutionary history of bats: fossils, molecules and morphology* (eds GF Gunnell, NB Simmons), pp. 317–352. New York, NY: Cambridge University Press.
- Adams RA. 2008 Morphogenesis in bat wings: linking development, evolution and ecology. *Cells Tissues Organs* **187**, 13–23. (doi:10.1159/000109960)
- Cooper KL, Tabin CJ. 2008 Understanding of bat wing evolution takes flight. *Gene Dev.* **22**, 121–124. (doi:10.1101/gad.1639108)
- Cooper LN, Cretekos CJ, Sears KE. 2012 The evolution and development of mammalian flight. *Rev. Dev. Biol.* **1**, 773–779. (doi:10.1002/wdev.50)
- Sears KE, Behringer RR, Rasweiler JJIV, Niswander LA. 2006 Development of bat flight: morphologic and molecular evolution of bat wing digits. *Proc. Natl Acad. Sci. USA* **103**, 6581–6586. (doi:10.1073/pnas.0509716103)
- Chen CH, Cretekos CJ, Rasweiler JJIV, Behringer RR. 2005 *Hoxd13* expression in the developing limbs of the short-tailed fruit bat, *Carollia perspicillata*. *Evol. Dev.* **7**, 130–141. (doi:10.1111/j.1525-142X.2005.05015.x)
- Weatherbee SD, Behringer RR, Rasweiler JJIV, Niswander LA. 2006 Interdigital webbing retention in bat wings illustrates genetic changes underlying amniote limb diversification. *Proc. Natl Acad. Sci. USA* **103**, 15 103–15 107. (doi:10.1073/pnas.0604934103)
- Hockman D, Cretekos CJ, Mason MK, Behringer RR, Jacobs DS, Illing N. 2008 A second wave of *Sonic hedgehog* expression during the development of the bat limb. *Proc. Natl Acad. Sci. USA* **105**, 16 982–16 987. (doi:10.1073/pnas.0805308105)
- Cretekos CJ, Wang Y, Green ED, Martin JF, Rasweiler JJIV, Behringer RR. 2008 Regulatory divergence modifies limb length between mammals. *Genes Dev.* **22**, 141–151. (doi:10.1101/gad.1620408)
- Wang Z, Han N, Racey PA, Ru B, He G. 2010 A comparative study of prenatal development in *Miniopterus schreibersii fuliginosus*, *Hipposideros armiger* and *H. pratti*. *BMC Dev. Biol.* **10**, 10. (doi:10.1186/1471-213X-10-10)
- Cretekos CJ, Weatherbee SD, Chen CH, Badwaik NK, Niswander L, Behringer RR, Rasweiler JJIV. 2005 Embryonic staging system for the short-tailed fruit bat, *Carollia perspicillata*, a model organism for the mammalian order Chiroptera, based upon timed pregnancies in captive-bred animals. *Dev. Dyn.* **233**, 721–738. (doi:10.1002/dvdy.20400)
- Wanek N, Muneoka K, Holler-Dinsmore G, Burton R, Bryant SV. 1989 A staging system for mouse limb development. *J. Exp. Zool.* **249**, 41–49. (doi:10.1002/jez.1402490109)
- Hockman D, Mason MK, Jacobs DS, Illing N. 2009 The role of early development in mammalian limb diversification: a descriptive comparison of early limb development between the natal long-fingered bat (*Miniopterus natalensis*) and the mouse (*Mus musculus*). *Dev. Dyn.* **238**, 965–979. (doi:10.1002/Dvdy.21896)
- Grabherr MG *et al.* 2011 Full-length transcriptome assembly from RNA-Seq data without a reference genome. *Nat. Biotechnol.* **29**, 644–652. (doi:10.1038/Nbt.1883)
- Haas BJ *et al.* 2013 De novo transcript sequence reconstruction from RNA-seq using the Trinity platform for reference generation and analysis. *Nat. Protoc.* **8**, 1494–1512. (doi:10.1038/nprot.2013.084)
- Li B, Dewey CN. 2011 RSEM: accurate transcript quantification from RNA-Seq data with or without a reference genome. *BMC Bioinformatics* **12**. (doi:10.1186/1471-2105-12-323)
- Wang Z, Young RL, Xue HL, Wagner GP. 2011 Transcriptomic analysis of avian digits reveals conserved and derived digit identities in birds. *Nature* **477**, 583–586. (doi:10.1038/Nature10391)
- Robinson MD, Oshlack A. 2010 A scaling normalization method for differential expression analysis of RNA-seq data. *Genome Biol.* **11**, R25. (doi:10.1186/gb-2010-11-3-r25)

19. Robinson MD, McCarthy DJ, Smyth GK. 2010 edgeR: a bioconductor package for differential expression analysis of digital gene expression data. *Bioinformatics* **26**, 139–140. (doi:10.1093/bioinformatics/btp616)
20. Wang L, Feng Z, Wang X, Wang X, Zhang X. 2010 DESeq: an R package for identifying differentially expressed genes from RNA-seq data. *Bioinformatics* **26**, 136–138. (doi:10.1093/bioinformatics/btp612)
21. Benjamini Y, Hochberg Y. 1995 Controlling the false discovery rate: a practical and powerful approach to multiple testing. *J. R. Stat. Soc. B* **57**, 289–300. (doi:10.2307/2346101)
22. Kawano H *et al.* 2004 Identification and characterization of novel developmentally regulated neural-specific proteins, BRINP family. *Mol. Brain Res.* **125**, 60–75. (doi:10.1016/j.molbrainres.2004.04.001)
23. Zakany J, Kmita M, Duboule D. 2004 A dual role for *Hox* genes in limb anterior–posterior asymmetry. *Science* **304**, 1669–1672. (doi:10.1126/science.1096049)
24. Zakany J, Duboule D. 2007 The role of *Hox* genes during vertebrate limb development. *Curr. Opin. Genet. Dev.* **17**, 359–366. (doi:10.1016/j.gde.2007.05.011)
25. Kmita M, Fraudeau N, Herault Y, Duboule D. 2002 Serial deletions and duplications suggest a mechanism for the collinearity of *Hoxd* genes in limbs. *Nature* **420**, 145–150. (doi:10.1038/nature01189)
26. Davis AP, Capecchi MR. 1994 Axial homeosis and appendicular skeleton defects in mice with a targeted disruption of *hoxd-11*. *Development* **120**, 2187–2198.
27. Boulet AM, Capecchi MR. 2002 Duplication of the *Hoxd11* gene causes alterations in the axial and appendicular skeleton of the mouse. *Dev. Biol.* **249**, 96–107. (doi:10.1006/dbio.2002.0755)
28. Davis AP, Capecchi MR. 1996 A mutational analysis of the 5' *HoxD* genes: dissection of genetic interactions during limb development in the mouse. *Development* **122**, 1175–1185.
29. Zakany J, Fromental-Ramain C, Warot X, Duboule D. 1997 Regulation of number and size of digits by posterior *Hox* genes: a dose-dependent mechanism with potential evolutionary implications. *Proc. Natl Acad. Sci. USA* **94**, 13 695–13 700. (doi:10.1073/pnas.94.25.13695)
30. Delpretti S, Zakany J, Duboule D. 2012 A function for all posterior *Hoxd* genes during digit development? *Dev. Dyn.* **241**, 792–802. (doi:10.1002/Dvdy.23756)
31. Fromental-Ramain C, Warot X, Lakkaraju S, Favier B, Haack H, Birling C, Dierich A, Doll EP, Chambon P. 1996 Specific and redundant functions of the paralogous *Hoxa-9* and *Hoxd-9* genes in forelimb and axial skeleton patterning. *Development* **122**, 461–472.
32. Wang Z, Dong D, Ru B, Young RL, Han N, Guo T, Zhang S. 2010 Digital gene expression tag profiling of bat digits provides robust candidates contributing to wing formation. *BMC Genomics* **11**, 619. (doi:10.1186/1471-2164-11-619)
33. Tarchini B, Duboule D, Kmita M. 2006 Regulatory constraints in the evolution of the tetrapod limb anterior–posterior polarity. *Nature* **443**, 985–988. (doi:10.1038/nature05247)
34. Liang L, Shen YY, Pan XW, Zhou TC, Yang C, Irwin DM, Zhang YP. 2013 Adaptive evolution of the *Hox* gene family for development in bats and dolphins. *PLoS ONE* **8**, e65944. (doi:10.1371/journal.pone.0065944)
35. Wang Z *et al.* 2009 Adaptive evolution of 5'*HoxD* genes in the origin and diversification of the cetacean flipper. *Mol. Biol. Evol.* **26**, 613–622. (doi:10.1093/molbev/msn282)
36. Ray R, Capecchi M. 2008 An examination of the Chiropteran *HoxD* locus from an evolutionary perspective. *Evol. Dev.* **10**, 657–670. (doi:10.1111/j.1525-142X.2008.00279.x)
37. Tumpel S, Sanz-Ezquerro JJ, Isaac A, Eblaghie MC, Dobson J, Tickle C. 2002 Regulation of *Tbx3* expression by anteroposterior signalling in vertebrate limb development. *Dev. Biol.* **250**, 251–262. (doi:10.1006/dbio.2002.0762)
38. Suzuki T, Takeuchi J, Koshiba-Takeuchi K, Ogura T. 2004 *Tbx* genes specify posterior digit identity through Shh and BMP signaling. *Dev. Cell* **6**, 43–53. (doi:10.1016/S1534-5807(03)00401-5)
39. Esmailpour T, Huang T. 2012 TBX3 promotes human embryonic stem cell proliferation and neuroepithelial differentiation in a differentiation stage-dependent manner. *Stem Cell* **30**, 2152–2163. (doi:10.1002/stem.1187)
40. Renard CA *et al.* 2007 *Tbx3* is a downstream target of the Wnt/beta-catenin pathway and a critical mediator of beta-catenin survival functions in liver cancer. *Cancer Res.* **67**, 901–910. (doi:10.1158/0008-5472.Can-06-2344)
41. Ito A, Asamoto M, Hokaiwado N, Takahashi S, Shirai T. 2005 *Tbx3* expression is related to apoptosis and cell proliferation in rat bladder both hyperplastic epithelial cells and carcinoma cells. *Cancer Lett.* **219**, 105–112. (doi:10.1016/j.canlet.2004.07.051)
42. Carlson H, Ota S, Song Y, Chen Y, Hurlin PJ. 2002 *Tbx3* impinges on the p53 pathway to suppress apoptosis, facilitate cell transformation and block myogenic differentiation. *Oncogene* **21**, 3827–3835. (doi:10.1038/sj.onc.1205476)
43. Govoni KE, Linares GR, Chen ST, Pourteymoor S, Mohan S. 2009 T-box 3 negatively regulates osteoblast differentiation by inhibiting expression of osterix and runx2. *J. Cell. Biochem.* **106**, 482–490. (doi:10.1002/jcb.22035)
44. Tanaka K, Matsumoto E, Higashimaki Y, Sugimoto T, Seino S, Kaji H. 2012 FAM5C is a soluble osteoblast differentiation factor linking muscle to bone. *Biochem. Biophys. Res. Commun.* **418**, 134–139. (doi:10.1016/j.bbrc.2011.12.147)
45. Kuroiwa T, Yamamoto N, Onda T, Shibahara T. 2009 Expression of the FAM5C in tongue squamous cell carcinoma. *Oncol. Rep.* **22**, 1005–1011. (doi:10.3892/or_00000528)
46. Chen L *et al.* 2012 Hypermethylated FAM5C and MYLK in serum as diagnosis and pre-warning markers for gastric cancer. *Dis. Markers* **32**, 195–202. (doi:10.3233/DMA-2011-0877)